

THE ELECTROCHEMICAL SYNTHESSES AND
CHARACTERIZATIONS OF NICKEL NANOPARTICLES
AND ZINC-NICKEL NANOALLOY ON COMPOSITE
GRAPHITE SUBSTRATE

RAMIN MOHAMMAD ALI TEHRANI

UNIVERSITI SAINS MALAYSIA

2009

THE ELECTROCHEMICAL SYNTHESSES AND
CHARACTERIZATIONS OF NICKEL NANOPARTICLES
AND ZINC-NICKEL NANOALLOY ON COMPOSITE
GRAPHITE SUBSTRATE

by

RAMIN MOHAMMAD ALI TEHRANI

Thesis submitted in fulfillment of the requirements
for the degree of
Doctor of Philosophy

October 2009

ACKNOWLEDGEMENT

Now, finishing this phase of study (Ph.D), in this part of my thesis, I am so pleased that I can express some words which are difficult to say directly. First of all, I thank God for bestowing health upon me to be able to think and for opening the way to gain knowledge. Besides, it is undeniable to consider my family's support, both financially and morally. I sincerely thank my parents, especially my mother and father.

I had never thought of coming to Malaysia for continuing study but it was my destiny to come to this country which brought me great blessings. It was not only worthwhile to reach for a higher knowledge and education but also a way to think appropriately, training in patience, effort, resistance, love, and gaining cognition and humility.

It is not an overstatement to say that this stage was the best evolution I have ever experienced in my life. Thanks to the merciful Allah, then I am indebted to warm and kind people of Malaysia, specially my dear respectable supervisor Associate Professor Sulaiman Ab Ghani. I never forget the second session I met him, expressing the word "Nanotechnology", which made me familiar with this new view in science. His attempt for great aims without being exhausted is admirable because he never stated his tiredness directly and in this way he showed me his insight. Prof. Sulaiman taught me how to be humble and pious despite of wealth, how to be inattentive to worldly life, and finally how to be kind and adore people.

I am so grateful to Assoc. Prof. Sulaiman who supported, advised and guided me and kept me motivated, spending his time momentarily in the school, even on weekends. I apologize for putting him in trouble, especially for

correcting my writings. Praying for him and the group members to be healthy and to live a long life successfully is the least I can do. I hope this relationship will continue constantly in future in order to make the opportunity for me to benefit of his knowledge.

Here I would like to express my gratitude to:

All the members in our research group

Honorable Dean of the School of Chemical Sciences, Professor Wan Ahmad Kamil

Honorable Deputies Dean especially Professor Bahruddin Saad and Dr. Afidah for supporting me to get the fellowship as well as all academic and technical staff of the School of Chemical Sciences

Gracious and kind staff of Chemical Sciences School's office

Kind staff of Electron Microscopy unit, the School of Biology especially Mr. Patchamuthu and Ms. Jamillah

Staff of Crystallography department and Nano-Optoelectronic Research and Technology Laboratory, the School of Physic

Ministry of Science, Technology and Invention (MOSTI), Malaysia for Fundamental Research Grant Scheme (FRGS) # 203/PKIMIA/671172

Executives of USM fellowship scheme

Friendly staff of the Institute of Graduate Studies (IPS)

Honorable Vice chancellor and their Deputies of USM

Ministry of education and Malaysia's Government for supporting and attracting foreign students

Most of all, I sincerely thank my wife for her great encouragement, patience and understanding during these years of my study.

TABLE OF CONTENTS

	Page
ACKNOWLEDGEMENTS	ii
TABLE OF CONTENTS	iv
LIST OF TABLES	viii
LIST OF FIGURES	ix
ABSTRAK	xiv
ABSTRACT	xvi
CHAPTER ONE : INTRODUCTION	1
1.1. Nanotechnology & nanoscience	1
1.2. Types and properties of nanostructures	2
1.3. Applications of nanomaterials	4
1.4. Nanoparticles (NPs)	4
1.4.1. Synthesis of NPs	4
1.4.2. Methods of NPs formation	6
1.4.3. Magnetic NPs	7
1.4.3.1. Nickel NPs	8
1.4.3.2. Properties and application of Ni NPs	9
1.4.3.3. Synthesize of Ni NPs	9
1.5. Nanoalloys	10
1.5.1. Zn-Ni alloy - properties and applications	11
1.5.2. Synthesis of Zn-Ni nanoalloy	12
1.6. Electrodeposition	12
1.6.1. Electrodeposition of NPs	12
1.6.1.1. Electrodeposition of Ni NPs	14
1.6.2. Electrodeposition of alloys	16
1.6.2.1. Electrodeposition of Zn-Ni nanoalloy	17
1.6.3. Hydrogen evolution reaction (HER)	22
1.7. Electrocristalization	22
1.7.1. Nucleation and growth phenomena	23

1.7.2.	Classical nucleation and growth mechanisms	23
1.7.3.	The heterogeneous nucleation mechanism using electrochemical methods	24
1.7.4.	Fast scan voltammetry deposition- Fast nucleation	25
1.8.	Fuel cells	27
1.8.1.	Basic principles	27
1.8.2.	Types of fuel cells	27
1.8.2.1.	Direct methanol fuel cells (DMFCs)	29
1.8.3.	Electrocatalytic oxidation of methanol by using Ni NPs	30
1.9.	Electrochemical sensors for clinical analysis	32
1.9.1.	Uric acid (UA)	32
1.9.2.	Determination of uric acid	33
1.10.	Objectives	35
CHAPTER TWO : EXPERIMENTATION		36
2.1.	Materials	36
2.2.	Electrochemical equipments	36
2.3.	Procedures	37
2.3.1.	Electrodeposition of Ni	37
2.3.2.	Electrodeposition of Zn-Ni	37
2.3.3.	Electrocatalytic studies	38
2.3.4.	Electrochemical sensor studies	38
2.4.	Characterization of nanomaterials	39
2.4.1.	Scanning electron microscope (SEM) / Electron disperse x-ray analysis (EDX)	39
2.4.2.	Transmission electron microscope (TEM)	40
2.4.3.	X-ray diffraction (XRD)	40
CHAPTER THREE : RESULTS AND DISCUSSION		42
3.1.	Linear fast scan voltammetry deposition technique	42
3.2.	Analysis of composite graphite substrate	42

3.3.	Electrodeposition of hcp Ni nanocrystal by fast scan voltammetry technique	44
3.3.1.	Linear sweep voltammetry	44
3.3.2.	Cyclic voltammetry	46
3.3.3.	Morphological characterization	51
3.3.4.	Structural analysis	68
3.3.5.	Composition analysis	75
3.4.	The catalytic properties of nano Ni modified CG (nano Ni/CG) electrode on methanol oxidation in alkaline medium	77
3.4.1.	Electrocatalytic oxidation of methanol	77
3.4.1.1.	Effect of scan rate	82
3.4.1.2.	Effect of particle size	85
3.4.1.3.	Effect of methanol concentration	87
3.4.2.	Stability of the modified electrode	90
3.5.	The Electroco-deposition of nanocrystalline single phase γ -Zn ₃ Ni alloy by fast scan voltammetry technique	94
3.5.1.	Electroco-deposition of Zn-Ni	94
3.5.2.	Cyclic voltammetry	98
3.5.3.	Morphological characterization	106
3.5.4.	Structural analysis	117
3.5.5.	Composition analysis	119
3.6.	The voltammetric detection of uric acid using nanocrystalline single-phase γ -Zn ₃ Ni alloy modified composite graphite electrode	122
3.6.1.	Electro-oxidation of UA on the nano- γ -Zn ₃ Ni/CG modified electrode	122
3.6.2.	Effect of pH	126
3.6.3.	Effect of scan rate	128
3.6.4.	Effect of ascorbic acid (AA)	130
3.6.5.	Calibration curve of UA	132
3.6.6.	Real sample analysis	134

CHAPTER FOUR : CONCLUSION AND RECOMMENDATION	137
REFERENCES	139
LIST OF PUBLICATIONS	168

LIST OF TABLES

	Page
1.1 Comparison of objects and distance	2
1.2 Typical nanomaterials	3
1.3 Summary of major differences of the fuel cell types	28
3.1 The parameters used to obtain the required nanocrystals diameter of Ni	65
3.2 Literature data for hcp Ni structural characteristics	72
3.3 Electrochemical parameters used in order to obtain the required particle size of Zn-Ni alloy nanoalloys	115
3.4 Determination of UA in urine samples using the modified electrode (n=3)	135
3.5 The comparison of different modified electrodes for sensing of UA	136

LIST OF FIGURES

	Page
1.1 Manipulation of carbon atoms and formation of new nanostructures	1
1.2 Top-down and bottom-up approach, to produce nanomaterials	5
1.3 Schematic representation of nanocrystal synthesis	26
1.4 The oxidation process of UA	34
3.1 (a) SEM and (b) EDX analyses of bare 2B pencil graphite composite	43
3.2 LSV of 5 mM NiCl ₂ + 1 M NH ₄ Cl, (a) and 1 M NH ₄ Cl (blank), (b) at scan rate 50 mVs ⁻¹ and pH 6	45
3.3 Cyclic voltammogram of Ni plating solution (5 mM NiCl ₂ in 1 M NH ₄ Cl) at pH 6 and scan rate 50 mVs ⁻¹ on a CG electrode	47
3.4 The deposition voltammogram of Ni nanostructure at 6500 mVs ⁻¹	49
3.5 SEM of Ni microcrystals obtained at different deposition potential but same deposition time; (A) -2.0 V, 420 s, (B) -1.7 V, 420 s and (C) -1.5 V, 420 s	52
3.6 SEM of Ni nanocrystals obtained at deposition potential -1.5 V but different deposition time; (A and B) 120 s in scale 200 and 100 nm respectively and (C) 90 s	55
3.7 SEM of Ni nanocrystals obtained at deposition potential -1.3 V and deposition time 420 s	58
3.8 TEM of Ni nanocrystals at deposition potential -1.4 V and deposition time 120 s	60
3.9 TEM of Ni nanocrystals at deposition potential -1.5 V and deposition time 120 s. The excerpts are enlargement at 20 nm, 50 nm and 100 nm	61
3.10 TEM of Ni nanocrystals at deposition potential -1.6 V and deposition time 120 s	63

3.11	The average size of Ni nanocrystals at various deposition potentials (deposition time 120 s)	64
3.12	The average size of Ni nanocrystals at various deposition times (deposition potential at -1.5 V)	64
3.13	TEM of Ni nanoparticles prepared at optimum condition of deposition potential and time but at various scan rates, (A) 3000 mVs ⁻¹ , (B) 5000 mVs ⁻¹ and (C) 8000 mVs ⁻¹	67
3.14	XRD pattern of Ni nanocrystal prepared at optimum condition	71
3.15	XRD pattern of Ni nanocrystal prepared at optimum condition but with longer deposition time (420 s)	74
3.16	EDX analysis and inset SEM of Ni nanocrystals at the optimum condition	
3.17	A) CVs of bare CG electrodes in the supporting electrolyte (0.1 M KOH), (a) and in the presence of 0.05 M methanol (b), (B) CVs of nanoNi/CG electrode in 0.1 M KOH (C) and in the presence of 0.05 M methanol (d). Scan rate 20 mVs ⁻¹	78
3.18	The dependency of anodic peak current to the square root of scan rate in 0.1 M KOH	81
3.19	(A) CVs response of nanoNi/CG electrode in 0.05 M methanol, at the following scan rates: (1) 10; (2) 20; (3) 50; (4) 100; (5) 200; (6) 400; (7) 500; and (8) 800 mVs ⁻¹ , (B) the dependency of anodic peak current to the square root of scan rate	84
3.20	(A) Cyclic voltammetric response of various Ni particles modified CG electrodes in 0.05 M methanol, with the following particle diameter: (1) 740 nm (prepared at -2.0 V); (2) 126 nm (prepared at -1.7 V); (3) 15 nm (prepared at -1.6 V); (4) 13.6 nm (prepared at -1.4 V) and (5) 9.7 nm (prepared at -1.5 V). (Deposition time 120 s). Scan rate 20 mVs ⁻¹ . (B) Effectiveness of electrode particle diameter in methanol oxidation calculated from above CV curves	86

3.21	Chronoamperograms obtained for nanoNi/CG electrode; (A) in the absence (1) and in the presence of (2) 0.01, (3) 0.02, (4) 0.03, (5) 0.04, (6) 0.05, (7) 0.08, (8) 0.1 and (9) 0.2 M methanol in the 0.1 M KOH using a potential step of 570 mV; and (B) the variations of currents measured against methanol concentrations	88
3.22	CV of hcp-nanoNi modified CG electrode in the 0.1 M KOH and 0.4 M methanol. Scan rate 20 mV s ⁻¹	89
3.23	The long-term cycle stability of the nanoNi/CG electrode for methanol oxidation	91
3.24	EDX analysis of the nanoNi/CG electrode after using as catalyst	93
3.25	LSV of various plating solutions at composite graphite. Scan rate 50 mVs ⁻¹	96
3.26	CV of (A) 5 mM Ni ²⁺ and (B) 10 mM Zn ²⁺ in 1.0 M NH ₄ Cl, pH 5.8. Scan rate 50 mVs ⁻¹	99
3.27	CV of Zn ²⁺ and Ni ²⁺ in 1.0 M NH ₄ Cl, pH 5.8 at scan rates (A) 50 mVs ⁻¹ , (B) 1000 mVs ⁻¹ and (C) the overlap of A and B. The (x, y) and (y') are supposed phases of Zn-Ni at low and high scan rate, respectively	101
3.28	The co-deposition voltammogram of Zn-Ni alloy at 10,000 mVs ⁻¹	103
3.29	CV of Zn-Ni alloy in 1.0 M NH ₄ Cl, pH 5.8, and scan rate 50 mVs ⁻¹ where the alloy is prepared at (A) low scan rate 100 mVs ⁻¹ and (B) ultra high scan rate 10,000 mVs ⁻¹	105
3.30	SEM of Zn-Ni particles obtained at various co-deposition applied potential (V) vs. Ag/AgCl, scan rate (mVs ⁻¹) and co-deposition time (s); (A) -1.7, 100, 420, (B) -1.7, 10,000, 420, (C) -1.6, 3000, 120, (D) -1.6, 6000, 120, (E)-1.6, 8000, 120, (F) -1.5, 10,000, 120, (G) -1.6, 10,000, 120 and (H) -1.6, 12000, 120	107
3.31	TEM of Zn-Ni nanoalloys obtained at scan rate of 10,000 mVs ⁻¹ ; (A) (with (B) enlargement and relevant histogram). Co-deposition applied potential and time are -1.6 V and 120 s respectively	112

3.32	TEM of Zn-Ni nanoalloys obtained at scan rates; (A) 1000 mVs ⁻¹ , (B) 6000 mVs ⁻¹ , (C) 8000 mVs ⁻¹ . For all images, co-deposition applied potential and time are at -1.6 V and 120 s respectively)	114
3.33	The dependence of Zn-Ni alloy nanoalloys size on the scan rate whilst nucleation potential and co-deposition time are at -1.6 V and 120 s respectively	116
3.34	The dependence of Zn-Ni alloy nanoalloys size on the co-deposition time whilst nucleation potential and scan rate are at -1.6 V and 10,000 mVs ⁻¹ respectively	116
3.35	The XRD of Zn-Ni alloy nanocrystals prepared at co-deposition potential – 1.6 V, time 120 s and scan rate; (A) 100 mVs ⁻¹ and (B) 10,000 mVs ⁻¹	118
3.36	The EDX and inset SEM of Zn-Ni alloy nanocrystals at co-deposition potential – 1.6 V, time 120 s and scan rate 10,000 mVs ⁻¹	120
3.37	The EDX and inset SEM of Zn-Ni alloy microcrystals at co-deposition potential – 1.6 V, time 120 s and scan rate 100 mVs ⁻¹	120
3.38	(A) Cyclic voltammograms of 0.2M PB solution (pH 7.0) on the; (a) bare CG and (b) nano- γ -Zn ₃ Ni/CG. (B) Cyclic voltammograms of 100 μ M UA in 0.2M PB (pH 7.0) on the; (c) unmodified CG and (d) nano- γ -Zn ₃ Ni. Scan rate 50 mVs ⁻¹	123
3.39	Mechanism for the electrochemical oxidation of uric acid	125
3.40	The pH dependence of 100 μ M UA in 0.2 M PB at the nano- γ -Zn ₃ Ni/CG electrode on (a) peak current and (b) peak potential	127
3.41	Cyclic voltammograms for the oxidation of 100 μ M UA in PB solution pH 7.0 at the nano- γ -Zn ₃ Ni/CG electrode with scan rates of (a) 20, (b) 50, (c) 100, (d) 150, and (e) 200 mVs ⁻¹ . Inset: plot of scan rate dependency of peak currents	129
3.42	Cyclic voltammograms of 100 μ M AA in PB solution (pH 7.0) on; (a) bare CG and (b) nano- γ -Zn ₃ Ni/CG electrodes. Scan rate 50 mVs ⁻¹	131

3.43	Chronoamperogram of successive additions of (a, b and d) 50, 100 and 400 μM AA, (c and e) 100 μM UA solutions in 0.2 M PB (pH 7.0) at 300 mV at the nano- $\gamma\text{-Zn}_3\text{Ni/CG}$ electrode	131
3.44	Typical differential pulse voltammogram of different concentrations of UA in PB solution (pH 7.0) at nano- $\gamma\text{-Zn}_3\text{Ni/CG}$. Concentration of UA (a to g):1, 5, 10, 20, 50, 100, and 200 μM . The corresponding calibration plot (inset). Pulse amplitude is 50 mV and step potential of 5 mV	133

SINTESIS DAN PENCIRIAN ELEKTROKIMIA NANOZARAH NIKEL DAN NANOALOI ZINK-NIKEL DI ATAS SUBSTRAT GRAFIT KOMPOSIT

ABSTRAK

Nanohablur nikel (Ni) dengan purata saiz 9.7 ± 2.3 nm dimendapkan ke atas komposit elektrod grafit daripada larutan saduran 5.0 mM $\text{NiCl}_2 \cdot 6\text{H}_2\text{O}$ dan 1.0 M NH_4Cl menggunakan kadar imbasan 6500 mVs^{-1} . Keupayaan mula $-1.5 \text{ V vs. Ag/AgCl}$, keupayaan akhir -0.5 V dan masa bekal 120 s telah digunakan bagi seluruh proses endapan. Kepelbagaian keupayaan bekal dan masa memberikan kesan terhadap ciri-ciri pemendapan nanohablur Ni. Ini termasuklah morfologi, garispusat, penyebaran dan bentuk struktur. Kajian ini telah menunjukkan bentuk struktur nanohablur Ni yang didapati sebagai hampir padat rapat heksagon (hcp).

Elektrod komposit grafit terubahsuai nanohablur hcp Ni (hcp-nano Ni/CG) telah disiasat bagi pengoksidaan bermangkin metanol dalam medium alkali menerusi peunbentukan NiOOH . Arus anodik yang tinggi telah didapati pada keupayaan puncak $+ 570 \text{ mV vs. Ag/AgCl}$. Kedua-dua, kadar imbasan dan kepekatan metanol memberikan kesan terhadap pengoksidaan metanol. Keputusan menunjukkan keaktifan pemangkin bertambah dengan pengurangan garispusat zarah Ni. Maka itu, elektrod terubahsuai adalah mangkin yang lebih cekap dalam pengoksidaan metanol.

Nanohablur fasa tunggal gamma aloi Zink–Nikel ($\gamma\text{-Zn}_3\text{Ni}$) telah diendapkan ke atas elektrod komposit grafit pada kadar imbasan $10,000 \text{ mVs}^{-1}$. Purata saiz zarah 11.8 ± 3.1 nm telah didapati. Analisis TEM menunjukkan keupayaan koendapan dikenakan iaitu keupayaan lampau pengnukleusan, kadar imbasan, dan masa koendapan adalah genting terhadap saiz hablur dan kandungan Ni dalam matriks. Voltammetri berkitar dan analisis XRD juga telah menunjukkan aloi fasa tunggal (γ -phase) sememangnya diperolehi pada

kadar imbasan yang digunakan. Keputusan juga menunjukkan nanozarah 19.0 wt. % Ni adalah seragam, terserakan dalam komposisi fasa salutan aloi.

CG terubahsuai nanoaloi γ -Zn₃Ni (nano- γ -Zn₃Ni/CG) telah digunakan untuk mengesan asid urik (UA) dengan teknik voltammetri. Elektrod terubahsuai tanpa enzim ini telah menunjukkan gerakbalas yang bagus dan spesifik terhadap pengoksidaan elektropemangkinan UA dalam penimbal 0.2 M fosfat (PB) (pH 7.0) pada +280 mV melawan Ag/AgCl berbanding dengan elektrod tidak terubahsuai pada +360 mV. Had pengesanan (S/N = 3) pada 0.2 μ M dan julat linear kepekatan daripada 1 hingga 400 μ M UA telah didapati. Kehadiran asid askorbik (AA) tidak mengganggu dalam penyukatan. Nano- γ -Zn₃Ni/CG telah digunakan untuk menentukan UA dalam sampel urin dan serum maanusia tanpa pra-pengolahan dengan keputusan yang memuaskan.

THE ELECTROCHEMICAL SYNTHESSES AND CHARACTERIZATIONS OF NICKEL NANOPARTICLES AND ZINC-NICKEL NANOALLOY ON COMPOSITE GRAPHITE SUBSTRATE

ABSTRACT

The nickel (Ni) nanocrystals with an average size of 9.7 ± 2.3 nm were deposited onto composite graphite electrode from a plating solution of 5.0 mM $\text{NiCl}_2 \cdot 6\text{H}_2\text{O}$ and 1.0 M NH_4Cl using scan rate of 6500 mVs^{-1} . The initial potential -1.5 V vs. Ag/AgCl , final potential -0.5 V and applied time 120 s were used for the whole deposition process. The variation of applied potentials and times has affected the characteristics of deposited Ni nanocrystals. It was found that the structural formation of Ni nanocrystals obtained were almost hexagonal close-packed (hcp).

The hcp nanocrystalline Ni modified composite graphite (hcp-nano Ni/CG) electrode was investigated for the catalytic oxidation of methanol in alkaline medium through the formation of NiOOH . A high anodic current was obtained at peak potential of $+570 \text{ mV}$ vs. Ag/AgCl . Both the scan rate and the methanol concentration affected the oxidation of methanol. The results showed that catalytic activity had increased with decreasing Ni particle size. Thus, the modified electrode was the most efficient catalyst in the oxidation of methanol.

The single phase gamma Zinc–Nickel alloy ($\gamma\text{-Zn}_3\text{Ni}$) nanocrystal was deposited on composite graphite electrode at a scan rate of $10,000 \text{ mVs}^{-1}$. The average particles size obtained was 11.8 ± 3.1 nm. The TEM analysis indicated that co-deposition applied potential, i.e. nucleation overpotential, scan rate, and co-deposition time were critical on crystals sizing and Ni content in the matrix. Cyclic voltammetry and analysis of XRD have also indicated that single phase (γ -phase) alloy was, indeed, obtained at the scan

rate used. The results also revealed that 19.0 wt. % Ni nanoparticles were, uniformly, dispersed in the phase compositions of the alloy coating.

The γ -Zn₃Ni nanoalloy modified CG (nano- γ -Zn₃Ni/CG) was employed for detection of uric acid (UA) by voltammetry techniques. This non-enzymatic modified electrode had an excellent response and specificity to the electrocatalytic oxidation of UA in 0.2 M phosphate buffer (PB) (pH 7.0) at +280 mV vs. Ag/AgCl as compared to an unmodified electrode at +360 mV. A limit of detection (S/N = 3) at 0.2 μ M and concentration linear range from 1 to 400 μ M UA were obtained. The presence of ascorbic acid (AA) did not interfere in the measurement. The nano- γ -Zn₃Ni/CG was used for the determination of UA in untreated human urine and serum samples with satisfactory results.

CHAPTER ONE

INTRODUCTION

1.1. Nanotechnology and Nanoscience

“Nanotechnology” is started by Nobel Laureate Physicist Richard Feynman, who stated in the 1959 lecture that “*there is plenty of room at the bottom*” [1] and the other is the approach of the self-assembly of molecular components, where each nanostructured component becomes part of a suprastructure.

“Nanoscience” involves the study and creation of materials, devices, and systems through the manipulation of individual atoms and molecules. For example, the formation of Fullerene, C_{60} , or Buckyballs and carbon nanotubes (CNTs) by rearranging carbon atoms in the graphite is shown in Figure 1.1.

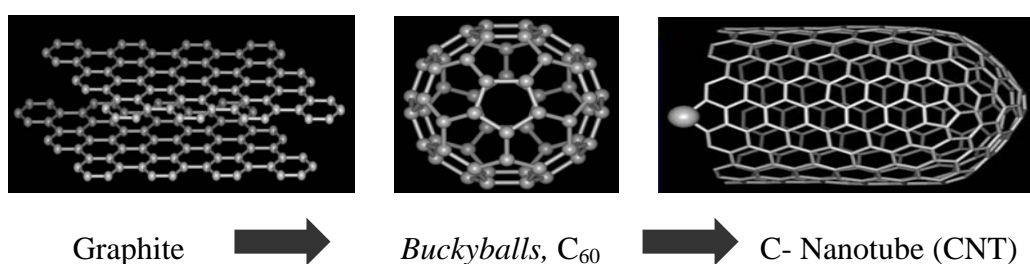


Figure 1.1 Manipulation of carbon atoms and formation of new nanostructures. (Images adopted from www.hkn.org/.../sp2006_goodnick_full.html). [Accessed 9th Feb 2009]

Nanoscience and nanotechnology primarily deal with the synthesis, characterization, exploration, and exploitation of nanostructured materials. These

materials are characterized by at least one dimension in the nanometer ($1\text{nm} = 10^{-9}$ m) range. Particles of size range 1-100 nm are considered nanoscale (Table 1.1). These nanomaterials, and structures and devices comprised of them, display unique mechanical, optical, electrical, and magnetic properties that differ radically from the corresponding bulk material [2].

Table 1.1 Comparison of objects and distance. [4]

Sample	Size (meters)
Uranium nucleus (diameter)	10^{-13}
Water molecule	10^{-10}
DNA molecule (width)	10^{-9}
protozoa	10^{-5}
Earthworm	10^{-2}
Human	2
Mount Everest (height)	10^3
Earth (diameter)	10^7
Distance from the Sun to Pluto	10^{13}

1.2. Type and properties of nanostructures

The nanomaterials cover various types of nanostructured materials including clusters, quantum dots, nanocrystals, nanowires, and nanotubes, while collections of nanostructures involve arrays, assemblies, and superlattices of the individual nanostructures [5,6]. Table 1.2 summarized the typical nanomaterials. The properties of materials with nanometer dimensions are significantly different from those of atoms and bulks materials. This is mainly due to the nanometer size of the materials which render them: (i) large fraction of surface atoms; (ii) high surface energy; (iii) spatial confinement; (iv) reduced imperfections, which do not exist in the corresponding bulk materials [7]. Due to their small dimensions, nanomaterials have

extremely large surface area to volume ratio, which makes a large fraction of atoms of the materials to be the surface or interfacial atoms, resulting in more surface dependent material properties.

Table 1.2 Typical nanomaterials. [5]

Structure	Size (approx.)	Materials
Nanocrystals and clusters (quantum dots)	diam. 1–10 nm	Metals, semiconductors, magnetic materials
Other nanoparticles	diam. 1–100 nm	Ceramic oxides
Nanowires	diam. 1–100 nm	Metals, semiconductors, oxides, sulfides, nitrides
Nanotubes	diam. 1–100 nm	Carbon, layered metal, chalcogenides
Nanoporous solids	pore diam. 0.5–10 nm	Zeolites, phosphates etc.
2–Dimensional arrays (of nanoparticles)	several nm– μm	Metals, semiconductors, magnetic materials
Surfaces and thin films	thickness 1–1000nm	A variety of materials
3–Dimensional structures (superlattices)	several nm in the three dimensions	Metals, semiconductors, magnetic materials

Especially when the sizes of nanomaterials are comparable to Debye length, the entire material will be affected by the surface properties of nanomaterials [8, 9]. This in turn may enhance or modify the properties of the bulk materials. For example, metallic nanoparticles can be used as very active catalysts. Chemical sensors fabricated from nanoparticles and nanowires have their sensitivities and selectivities enhanced. The nanometer feature sizes of nanomaterials also have spatial confinement effect on the materials, which bring the quantum effects. Nanoparticles can be viewed as a zero dimension quantum dot while various nanowires and nanotubes can be viewed as quantum wires.

1.3. Applications of nanomaterials

There is continuing interest in nanomaterials because of potential applications in fields such as catalysis, sensors, coatings, semiconductor, fuel cells, drug delivery and others [3, 10-13].

1.4. Nanoparticles (NPs)

NPs are aggregates of between a few and many millions of atoms or molecules. They may consist of identical atoms, or molecules, or two or more different species [13].

Interest in NPs arises, because they constitute a new type of material which may have properties which are distinct from those of individual atoms and molecules or bulk materials. An important reason for the interest in NPs and clusters is the size-dependent evolution of their properties, such as their structures [14, 15].

1.4.1. Synthesis of NPs

There are two different approaches to synthesize NPs: top-down and bottom up as shown in Figure 1.2.

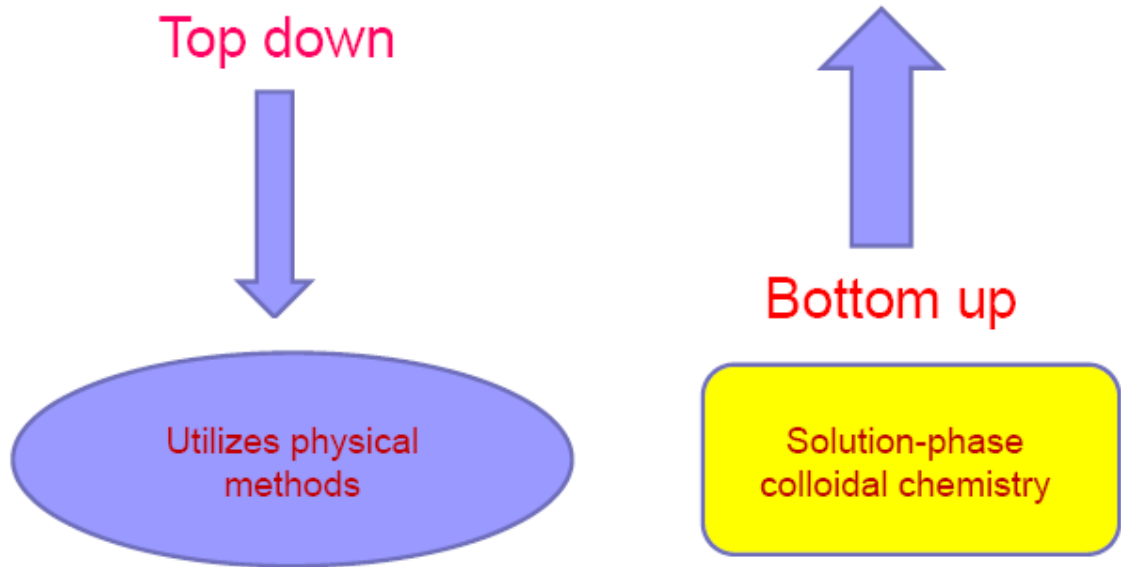


Figure 1.2 Top-down and bottom-up approach, to produce nanomaterials.

The advantage of the top down is it can produce large quantity of NPs but uniformed –sized nanocrystals and size control is very difficult to be achieved. In the bottom up uniform NPs with controlled particle size can be produced and various shaped nanocrystals including nanorods and nanowires can be obtained by varying the reaction conditions such as temperature, concentrations or the types of surfactants.

Solution chemical routes often provide the best method for production of NPs due to homogeneity from the molecular level design of the materials. Solution routes also allow control of particle size and size distribution, morphology, and agglomerate size through the individual manipulation of the parameters that determine nucleation, growth, and coalescence [3, 4, 7].

1.4.2. Methods of NPs Formation

Several routes have been investigated to obtain metal NPs including chemical reduction [16-18], sol-gel processes [5, 19] supercritical fluid deposition [20, 21], adsorption-precipitation [22], sonochemistry [5] electrochemical deposition [5, 7, 23], physical vapor deposition (PVD), chemical vapor deposition (CVD) [5, 7], hydrothermal [24], arc discharge [25] and electroless plating. [26]. Although the use of many such techniques is limited to laboratory scale, but, electrodeposition, inert gas condensation and mechanical alloying, are among the methods that are available for commercial uses [27].

1.4.3. Magnetic NPs

At finite sizes magnetic NPs will begin to exhibit unique electrical, chemical, structural, and magnetic properties with potential applications including: information storage, color imaging, magnetic refrigeration, and ferrofluids differing from the bulk material. In a magnetic particle, the magnetic moment is held along a certain direction within the structure by the magnetic anisotropy [28, 29].

Transition metallic materials such as the ferromagnetic metals Ni, Fe and Co have been extensively studied because of their wide range of application due to their potential in transformers, inductive devices, medical imaging, catalysis etc. Additionally, the development of uniform magnetic NPs is typically an important issue in ultrahigh-density magnetic storage devices and sensors [14, 30].

1.4.3.1. Nickel NPs

Nickel (Ni) is a lustrous white, hard, with ferromagnetic properties in transition metal group VIII of the Periodic Table. It has high ductility, good thermal conductivity, high strength and fair electrical conductivity [31]. Ni is an important metal commercially because of its resistance to corrosion in strongly alkaline environment. Hence, it is used as electrode for water electrolysis in alkaline solutions [32].

The physico-chemical properties of the Ni NPs are very different from the bulk Ni crystals. An example of this is the high surface area and excellent magnetic properties of ferromagnetic Ni nanocrystals which has attracted considerable attention than the bulk Ni [33].

1.4.3.2. Properties and application of Ni NPs

Ni NPs have highly magnetic properties with magnetic moment μ per atom that exceed the bulk value of 0.61μ per atom due to surface-enhanced magnetism [33]. Ni NPs below 100 nm have attracted considerable interest in recent years due to their applications as catalysis superconductors, electronic, optical, mechanical devices, magnetic recording media, magnetic sensors and biomolecular separations [34–38]. Ni is an effective and cheap catalyst for oxidation of organic compounds particularly, methanol and ethanol in alkaline media [39-43].

Natural Ni crystallizes into face-centered cubic (fcc) [44-46] and Ni nanoparticles with hexagonal close-packed (hcp) structure, however, is rare due to the difficulties in synthesizing the hcp Ni [47]. The fcc and hcp Ni NPs have, remarkably, similar magnetic moment at 0.59 and $0.60 \mu_B$, respectively [48]. However, the hcp formation is anti-ferromagnetic and paramagnetic whereas the fcc formation is ferromagnetic and super paramagnetic. The difference in magnetic state of the metastable hcp Ni nanocrystals is due to the increase in bond distance (2.665 \AA) as compared to the bond distance (2.499 \AA) of the stable fcc Ni nanocrystals [49].

Nonetheless, this divergence is capitalized in spintronic and recording applications whereby a large uniaxial anisotropy is preferred [50].

1.4.3.3. Synthesis of Ni NPs

A variety of techniques have been used to produce fcc Ni NPs, such as chemical reduction [51-55], sonochemical deposition [56], sol-gel [57] pyrolysis [32, 58], electroless [26], sputtering [59], hydrothermal reduction [60] CVD of metal into the nanopores of template materials [61], pulsed electrodeposition [62, 63] and direct electrodeposition [64]. In addition, use of additives such as saccharin and sodium lauryl sulphonate through pulse plating has been reported [65-67]. A mixture of fcc and hcp Ni nanocrystals have been produced through laser decomposition in the gas phase and sol-gel techniques [47, 68].

1.5. Nanoalloys

The term alloy nanoclusters or “nanoalloys” have been coined to describe the assembly of the materials with well-defined, controllable properties and structures on the nanometer scale coupled with the flexibility afforded by intermetallic materials. Nanoalloys are of interest for catalysis (e.g. catalytic converters in automobiles and fuel cell electrodes), electronic, magnetic, sensors and biomedical applications (e.g. biosensors). Chemical and physical properties can be tuned by varying cluster size, composition and chemical ordering. As finite size effects, it may display properties

distinct from bulk alloys (*e.g.* Ag and Fe are miscible in clusters but not in bulk alloys).

Bimetallic nanoalloys (A_mB_n) can be generated in a variety of methods (*e.g.* chemical reduction, thermal decomposition of transition metals, electrochemical synthesis, sonochemical synthesis, ion implantation, etc.), in solution, in the gas phase, supported on a substrate, or in a matrix with, more or less, controlled size ($m + n$) and composition (m/n). Many of the methods and media for studying nanoalloys are the same as for pure monometallic nanoparticles, though there may be added complexities [13, 14, 69].

Much attention has focused on nanoalloys formed between catalytic metals (Ni, Pd, Pt) and transition metals (Cu, Ag, Zn and Au) since the alloying can dramatically alter the surface structure, composition, and reactivity of the catalyst [70].

1.5.1. Zn-Ni alloy - properties and applications

Usually the mechanical and chemical properties of metals are improved by alloying. In particular, it is known that the mechanical properties of Zn electrodeposits can be improved by alloying Zn with Ni [71, 72]. Also, the requirements for metallic coatings especially in automobile industry with a corrosion resistance better than that of pure Zn have led to production of electrodeposits based on Zn alloys with metals of the eight group (Zn–Ni, Zn–Co, and Zn–Fe) [73-75]. Zn–Ni coatings are likely to have better anti-corrosion properties [76-78]. Moreover,

deposits of Zn–Ni are a pollution-free coating alternative to cadmium [71, 76]. There are three intermetallic phases, i.e. γ , η and δ based on Ni content, on the equilibrium phase diagram for the Zn-Ni binary system [79, 80]. The γ -phase Zn_3Ni or $Zn_{21}Ni_5$ alloy has 15 – 26 wt. % Ni whilst the δ -phase Zn_8Ni or $Zn_{22}Ni_3$ alloy has 10 – 15 wt. % Ni [79]. Alloys of less than 10 wt. % Ni are mixture of γ and η phases [81]. However, for the vast majority of industrial applications, the single γ -phase alloy is the one of interest [81]. The highest Ni content (15–22 wt.%) commonly employed in the aeronautical industry [76]. The phases formation of Zn-Ni alloy depends on deposition conditions such as the current density (I_c), deposition potential (E_c), the ratio of $[Zn^{2+}] / [Ni^{2+}]$ in electrolyte, temperature and etc. By increasing the E_c value and/or current density (I_c) the γ -phase becomes dominant in the alloy [81-83]. On the other hand, by increasing temperature (max at 60 °C) Ni content is increased [84, 85].

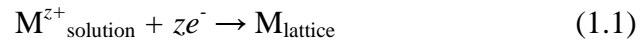
1.5.2. Synthesis of Zn-Ni nanoalloy

For a long time, electrodeposition has been known as a simple and cheap process available for the preparation of decorative and protective coating of metals and alloys. This process has been used to prepare several bimetallic alloy especially Zn–Ni [86]. For the synthesis of Zn-Ni nanoalloy via the electrodeposition technique, please see section 1.6.2.1.

1.6. Electrodeposition

Electrodeposition is the process of forming a film or a bulk material using an electrochemical process where the electrons are supplied by an external power supply. A three-electrode electrochemical cell usually contains a reference electrode, a specially designed cathode, and an anode or counter electrode [87, 88].

In general, in electrodeposition, a conductive electrode (substrate) is in contact with an aqueous ionic solution. The deposition reaction which is presented by Eq. (1.1) is a reaction of charged particles at the interface between a solid conductive electrode and a liquid solution. The two types of charged particles, a metal ion and an electron, can cross the interface.



Four types of fundamental subjects are involved in the process represented by Eq. (1.1): (1) metal–solution interface as the locus of the deposition process, (2) kinetics and mechanism of the deposition process, (3) nucleation and growth processes of the metal lattice (M_{lattice}) and (4) structure and properties of the deposits [89].

1.6.1. Electrodeposition of NPs

The electrodeposition provides a multipurpose method for producing metal NPs and nanowires with control electrochemical parameters [90, 91]. The obvious advantages of this century-old process of electrodeposition for synthesis of

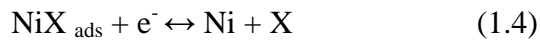
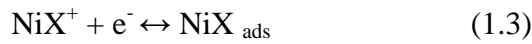
nanostructure materials are the rapidity, low cost, free from porosity, high purity, industrial applicability, potential to overcome shape limitations or allows the production of free-standing parts with complex shapes, higher deposition rates, production of coatings on widely differing substrates, ability to produce structural features with sizes ranging from nm to μm , easy control over alloy composition, ability to produce compositions unattainable by other techniques and the possibility of forming of simple low-cost multilayers in many different systems, such as Cu/Ni, Ni/Ni-P, Ni-Zn [92].

A more general method to suspend particle expansion is the regulation of the electrodeposition parameters; current or voltage. A two step procedure is employed; a high overpotential is applied for a short period to nucleate metal particles at the surface. Then to slowly grow the particles to the required final dimension a low overpotential pulse is applied. The low overpotential promotes a modest variation in particle size [93]. The shape of the particles produced by electrodeposition depends on the substrate (working electrode) employed and the applied overpotential. Metal; including gold, silver and Ni [87, 94, 95], with spherical geometry have been prepared on graphite planes. Also on graphite substrate, spherical NPs are formed when a high overpotential is employed [62]. At low energy surfaces (e.g. H-terminated silicon, graphite and highly oriented pyrolytic graphite (HOPG)), metal particles are promptly formed and the size distribution of these particles becomes monotonically broader during the deposition [91, 96].

1.6.1.1. Electrodeposition of Ni NPs

Ni deposition has been widely studied and much work has been devoted to the mechanism of the deposition process. The properties and structures of the electrodeposits are closely related to the electrolyte composition and electroplating parameters.

A survey of the reaction mechanism, as well as the kinetics of Ni NPs electrodeposition from different baths, is given by Saraby-Reintjes and Fleischmann [97]. The generally accepted mechanism involves two consecutive one-electron charge transfers with the formation of an adsorbed cationic Ni-containing complex. This mechanism can be represented as:



The anion X is assumed to be OH^- , SO_4^{2-} or Cl^- [97-99].

The first true effort to use electrochemical route in producing metallic NPs is by Reetz and Helbig [100]. Tejon and Chen [101], El-Sherik and Urb [102] and Moti *et al.* [103] studied the process for producing nanocrystalline Ni having grain sizes in the range of 10 – 40 nm, 30-40 nm and 14-28 nm respectively by pulse electrodeposition from a modified Watts-type bath. The solution consists of Ni sulfate, Ni chloride, boric acid and saccharin inhibitor ($\text{C}_7\text{H}_4\text{NO}_3\text{S}$). Ni NPs with a grain size of about 30 – 50 nm, have been obtained by direct current

electrodeposition [67, 104-110]. In another method Ni NPs electrodeposited in presence of a magnetic field has a fine grain structure from 17 to 25 nm [111]. In this method the magneto electrolysis was carried out at current density of 10 mA cm^{-2} for 1 h. A direct electrodeposition of Ni NPs by applying a constant current density of 10 mA cm^{-2} onto the Ni substrate has produced particles with diameter of about 40 nm [112].

Although the literature on Ni electrodeposition is voluminous but research on the preparation of Ni NPs with size below 50 nm by voltammetry techniques, especially, on composite graphite electrode, however, are scarce. Zach and Penner in 2000 [62] have used potentiostatic pulse technique on graphite surfaces to produce Ni NPs with grain size of 20 to 600 nm in diameter. In another report [64] Ni and its companion NiO are electrodeposited on multi-walled carbon nanotubes (MWCNT) through molecular level design and cyclic voltammetry method. The sizes of both NiO and Ni nanoparticles are $1.0 \mu\text{m}$ and 8 nm respectively. Recently (in 2005), Atashbar *et al.* [113] have reported the synthesis of Ni nanowires on freshly cleaved surface of highly oriented pyrolytic graphite (HOPG) by cyclic voltammetry technique with average particles size of approximately 15 nm.

The rather low value of the Gibbs energy (ΔG) of nuclei formation anticipates a strong tendency of Ni to nucleate on the carbon surface in the aqueous plating solution of NiCl_2 [114].

The electrodeposition of Ni and its alloys from aqueous solutions can be complicated by the hydrogen evolution reaction (HER) which depends on pH [115].

The electrodeposition of Ni and HER on the graphite occurs in the negative applied potential or nucleation overpotential [62]. Thus, the electrocatalytic activity of Ni obtained in the process is advantageous for HER [66, 116].

1.6.2. Electrodeposition of alloys

This is the simultaneous deposition of more than one metal. The characteristics of metallic alloys, tensile strength, ductility, magnetic property, corrosion resistance, and catalytic property, are markedly influenced by alloying and are quite different from those of single metals. Because of that, in some applications the alloys replace the single metal. In alloy and compound electrodeposition, the equilibrium potentials of the alloy or compound components, the activities of the ions in solution, and the stability of the resultant deposit all are important thermodynamic considerations. For a compound M_nN_m , the conditions necessary to obtain the simultaneous deposition of two different kinds of ions at the cathode is:

$$E_M + \eta^m = E_N + \eta^n \quad (1.5)$$

where E_M and E_N are the respective equilibrium potentials of M and N, η^m and η^n are the over potentials required for electrodepositing M and N, respectively. Considering the fact that the activities of the metals M and N in the compound or alloy are determined by their concentrations in the solution and by the thermodynamic stability of the deposit, and often vary during deposition, it is very difficult to control

deposit stoichiometry. In addition, the control of ionic strength and solute concentration are important for uniform deposition.

For the growth of films by electrodeposition, a few practical concerns need to be addressed. Though aqueous solutions are often used, due to electrolysis of water nonaqueous solvent or molten salts are sometime used. The electrical conductivity of the deposit must be high enough to permit the deposition of successive layers. The electrodeposition is therefore applied only for the growth of metal, semiconductors and conductive polymer films. Deposition can be accomplished at constant current or constant potential, or by other means, such as involving pulsed current or voltage and post treatment may be employed to improve the characteristics of the deposits [7, 117].

Alloy formation by electrochemical co-deposition of two metal ions in aqueous electrolytes in the overpotential deposition regions of both metals such as Cu-Ni, Zn-Co, and Zn-Ni and also in both the underpotential deposition region of a less noble metal and the overpotential deposition region of another noble metal has been investigated extensively [117].

1.6.2.1. Electrodeposition of Zn-Ni nanoalloy

The electrodeposition of Zn-Ni alloys is classified by Brenner [118] as an anomalous co-deposition, where zinc, which is the less noble metal, deposits preferentially. The formal electrode potentials (E°) for Zn^{2+}/Zn and Ni^{2+}/Ni pairs are - 0.762 V and - 0.236 V, respectively. The alloy composition is always in abundance

of Zn rather than of Ni. Because of this anomalous co-deposition behavior, alloys with high Ni content can be difficult to obtain from aqueous plating baths. A higher Ni content would lead to a more positive open-circuit potential, which in turn reduces the motivation force for the galvanic corrosion [119]. Attempts to rationalize the anomalous electrodeposition of the Zn-Ni alloy are not quite successful [120-122]. A reason could be due to the favorable kinetic effect of Zn deposition as compared to Ni deposition [120]. The increases in pH near the cathode surface followed by the formation of Zn hydroxide precipitate and the inhibition of Ni discharge have also been suggested [121, 122]. In addition to this, the effects of organic additives on improved Ni content in the alloy composition have also been investigated [120, 124].

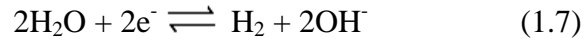
With the rapid development of nanoscience and nanotechnology, investigating the preparation, structures, and properties of ferromagnetic-nonmagnetic nanoalloys stimulates much more interest. Nanoalloys can be electrodeposited and could be potential candidates for magnetic recording and other applications in electronic industry; but this requires films with very good quality, reproducible composition and nanostructure [75, 123]. However, reports on the Zn-Ni nanoalloys and its applications especially in other areas except in the corrosion studies are rare. There are some indications in the literature that Zn-Ni alloys may be synthesized in the nanostructure [85, 125-127]. Benballa *et al.* [128] has obtained nanocrystalline Zn-Ni coatings from the ammonium chloride baths. Brooks and Erb [125] have used pulse current electrodeposition to synthesize nanocrystalline γ - phase $\text{Ni}_5\text{Zn}_{21}$ alloy with a wide spectrum of grain size ranging from 15 μm – 20 nm. Liu *et al.* [124] has reported the synthesis of Zn-Ni alloy nanowires of 60 nm

diameters through template-assisted electrochemical deposition method. Recently, Zn–Ni alloy nanorods with diameter about 65 nm electrodeposited in the nanopores of aluminium oxide have been reported by Foyet *et al.* [123]. By manipulating the plating parameters the grain size can be changed in the range 15 - 20 nm, in correspondence the alloy composition varies in the ranges 9-18 wt.% Ni [129, 130]. However, the fabrication of single phase γ – Zn–Ni alloy nanocrystalline with average size of less than 20 nm using cyclic voltammetry has not yet been reported.

1.6.3. Hydrogen evolution reaction (HER)

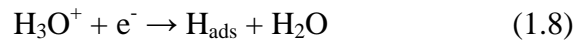
It is one of the most common electrochemical reactions in which hydrogen gas is produced at the cathode of an electrolysis cell by the reduction of hydrogen ions or by the reduction of the water molecules of an aqueous solution. The cathodic hydrogen evolution starts, at a more negative potential, whereas at more positive potentials, oxygen is evolved anodically. Its special characteristic is the fact that it can proceed in any aqueous solution; particular reactants need not be added [131, 132]. The HER is of great scientific and technological importance. Technological importance stems from the fact that for example, electrodeposition of some metals, such as Ni and Cr, is accompanied by simultaneous hydrogen evolution. Viewed electrochemically when metal deposition is accompanied by hydrogen evolution, it may be said that one deals with alloy plating in which hydrogen is the codepositing element (H₂ co-evolution) [62, 89, 133].

The overall reactions of hydrogen evolution in an acid solution and in neutral and basic media are:



The mechanism of this process and the overpotential depend on the electrode material. Cathodic hydrogen evolution is a complex two-electron reaction occurring through several consecutive, simpler intermediate steps. Each of these steps is sometimes referred to with the name of the scientist who had suggested that it was rate determining for the overall reaction; the steps are [89, 134]:

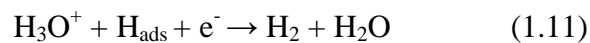
Step 1: The discharge (*Volmer*) step,



Step 2a: The recombination (*Tafel*) or chemical desorption step,



Step 2b: The electrochemical desorption (*Heyrovsky*) step,



In 1905, Julius Tafel put forward the opinion that the “recombination step” is rate determining while the discharge step is in equilibrium [131]. The physical basis of

this theory is the fact that the recombination of two atoms will not occur instantaneously (in every collision) but with some finite, low rate. According to Gileadi [135], for metals that are good catalysts for the HER, the Tafel reaction is the rate determining step at low overpotentials, while at higher overpotentials the Heyrovsky mechanism becomes the rate determining step. The Volmer reaction is the rate determining step at very high overpotentials. Normally, the Volmer reaction is followed either by the Tafel or by Heyrovsky reaction. It is concluded that the HER follows a Volmer-Heyrovsky mechanism at high overpotential.

In situ spectroscopic techniques and other methods such as cyclic voltammetry give definitive evidence for the formation of adsorbed hydrogen atoms on some metals, particularly the platinum metals. Early studies [136, 137] showed that the rate constants of the HER reach a maximum with the platinum group metals, but that Ni-based electrodes are also very active electrocatalysts for the HER [65].

For such metals, the exchange current density for H₂ evolution is relatively high. For other metals (e.g. Pb, Cd, and Hg), there is no evidence for adsorbed intermediates and the exchange current densities are low, i.e., a very large overpotential is needed in order to see significant H₂ evolution. Whatever the mechanism is, the formation and then the cleavage of an M–H bond will be involved in the reaction. Thus the maximum rate of hydrogen evolution will occur at intermediate values of metal-hydrogen bond strength, which leads to a significant, but not complete monolayer, covered by adsorbed hydrogen atoms [132, 133].

1.7. Electrocrystalization

1.7.1. Nucleation and growth phenomena

Metal electrodeposition takes place at the boundary between two phases, an electronic conductor such as a metal or substrate and an electrolyte solution. The charge carriers in this phase are ions and under certain conditions the ions in the region close to the electronic conductor may exchange electrons with it. It is, namely, during the interfacial charge transfer that electrochemical nucleation occurs [138, 139].

Essentially, the preparation of nanocrystals is a process of electrocrystallization of metal on electrode surface which is directly related to nucleation and crystal growth [139]. The mechanism of nucleation includes *instantaneous* and *progressive* nucleation [140, 141] and the direction of nucleation includes two-dimensional (2D) and three-dimensional (3D) growth [142]. In the instantaneous nucleation mode, the number of nuclei on the surface is instantaneously saturated, and all reaction sites are activated at the same time. In the progressive nucleation mode, the number of nuclei on the surface is less than the saturation nuclear number density, and new nuclei continue to form progressively [27, 114, 143, 144]. In instantaneous nucleation, the growth rate of a new phase is high but the number of formed active nucleation sites is low. On the other hand, the progressive nucleation is slow, but occurs on a large number of active sites [114]. In fact, the instantaneous nucleation corresponds to a slow growth of nuclei on a small number of active sites where progressive nucleation corresponds to fast growth of

nuclei on many active sites [143]. The higher the nucleation rate during deposition, the finer are the crystal grains of the deposit. Normal crystal grains for example a fibrous structure are obtained at higher growth rate on the substrate surface. The forms of the growing crystals determine the general appearance and structure of the deposit [139].

In the fabrications of nanostructured materials by electrochemical deposition, new phase formation [145] involves so many parameters and thus practical aspects of this method have to be considered [146]. These includes the nucleation and growth mechanism at underpotential deposition (UPD) [147] or overpotential deposition (OPD) conditions, nature of the substrate and its specific free surface energy, the occurrence of surface alloying phenomena, concentration of electrolyte, etc. [27, 139, 142, 143, 146, 148]. The final size distribution of the electrodeposits, however, strongly depends on the kinetics of the nucleation and growth [27]. It is possible to create a small number of nuclei by applying a short pulse of a voltage above threshold or a short overpotential η that is large enough. So that it can initiate nucleation on substrate surface [93, 148]. The effect of different nucleation and growth mechanisms on the morphology of 3D nanostructures or nanocrystals has been demonstrated in Ni overpotential deposition [138, 146].

1.7.2. Classical nucleation and growth mechanisms

The basic thermodynamic concepts of nucleation and crystal growth were formulated in the pioneering works of Gibbs in 1878 in his remarkable study on the equilibrium of heterogeneous systems [139, 146]. The heterogeneous nucleation is

generally referred to “Island or Volmer-Weber” growth [149]. Other two nucleation-modes are “Layer or Frank-van der Merwe” growth and “Island-layer or Stranski-Krastanov” growth [7, 143]. Island growth occurs when the growth species are more strongly bonded to each other than to the substrate. Electrodeposition on substrates with low surface energy, such as highly oriented pyrolytic graphite (HOPG), graphite and mica substrates display this type of nucleation during the initial film deposition, i.e., a three-dimensional (3D) island growth mode, leading to nanoparticle formation [7, 150].

The layer growth is the opposite of the island growth, where growth species are equally bound more strongly to the substrate than to each other. First a complete monolayer is formed, before the deposition of a second layer occurs. The most important examples of layer growth mode are the epitaxial growth of single crystal films. The island-layer growth is an intermediate combination of layer growth and island growth. Such a growth mode typically involves the stress, which is developed during the formation of the nuclei or films [7].

1.7.3. The heterogeneous nucleation mechanism using electrochemical methods

Use of electrochemical methods in the heterogeneous nucleation has some advantages over the other methods. The major one is that the driving force for the nucleation can be precisely and conveniently controlled by varying nucleation potential. Nucleation and growth can be broadly classified into two categories: ‘interfacial (or charge) controlled’, in which the rate of the process is determined by the rate of incorporation of electroactive species into the new phase, and ‘diffusion